The current issue and full text archive of this journal is available at
www.emeraldinsight.com/0961-5539.htm

Geometrical and Rayleigh number effects in the transient laminar free convection between two vertically eccentric spheres

Mamadou Lamine Sow, Joseph Sarr, Cheikh Mbow and Babacar Mbow
Department of Physics, Faculty of Science and Technology, University Cheikh Anta Diop of Dakar, Fann, Senegal
Bernard Claudet
Department of Physics, Faculty of Exact and Experimental Sciences, University of Perpignan, Perpignan, France, and
Mamadou Mansour Kane
Centre for Study and Research in Renewable Energy (CERER), University Cheikh Anta Diop of Dakar, Hann Equipe, Senegal

Received 12 April 2006
Revised 28 March 2007
Accepted 28 March 2007

Abstract

Purpose – The purpose of this paper is to study the transient natural convection of a Newtonian fluid which develops in a closed spherical annulus delimited by two vertically eccentric spheres by using a bispherical coordinates system. The inner sphere is heated by a heat flux of constant density and the outer one is maintained isothermal.

Design/methodology/approach – The transfer equations are written by using a bispherical coordinates system. The Navier-Stokes equations are solved and coupled with the energy equation by using the alternating direction implicit (ADI) and the successive over relaxation (SOR) methods.

Findings – The study of the stream function and the Nusselt number shows that the convection motion is reinforced for the geometries characterized by positive values of the eccentricity with heat exchange increasing. The Nusselt number increases with the modified Rayleigh number. The heat exchange increases with the radius ratio. The results show that the steady state is reached faster when the modified Rayleigh number increases and the influence of the eccentricity is very low on the establishment of the steady state. The fluids flow depends strongly on the eccentricity and the modified Rayleigh number.

Research limitations/implications – Simulations are performed for modified Rayleigh numbers ranging from 10^3 to 10^6, for eccentricities varying between –0.6 and +0.6 and for radius ratio between 1.5 and 2.

Originality/value – The results of eccentricity and modified Rayleigh number effects in transient natural convection between vertically eccentric spheres have been displayed.

Keywords Convection, Heat, Flux, Flow, Laminar flow
Paper type Research paper

Nomenclature

Latin letters

a = parameter of torus pole [m]

D = hydraulic diameter, $D = r_i - r_e$ [m]

e = eccentricity, $e = \frac{\overline{O_i O_e}}{D}$

g = gravitational acceleration [$m\,s^{-2}$]

G_1 and G_2 = coefficients, $G_1 = G_1(\eta, \theta) = \frac{1 - \cos\theta \mathrm{ch}\eta}{\mathrm{ch}\eta - \cos\theta}$ and $G_2 = G_2(\eta, \theta) = -\frac{\sin\theta \mathrm{sh}\eta}{\mathrm{ch}\eta - \cos\theta}$

International Journal of Numerical Methods for Heat & Fluid Flow
Vol. 19 No. 5, 2009
pp. 689-704

0961-5539
DOI 10.1108/09615530910963599

Gr = modified Grashof number, $Gr = \frac{Ra}{Pr}$

H, K = dimensionless parameters, $H = \frac{a}{D(ch\eta - \cos\theta)}$ and $K = \frac{a \sin\theta}{D(ch\eta - \cos\theta)}$

Nu = Nusselt number, $Nu = \frac{q^*_{cond} + q^*_{conv}}{q^*_{cond}}$

O = sphere centre

Pr = Prandlt number, $Pr = \frac{\nu}{\alpha}$

q = heat flux density [W m^{-2}]

q* = heat flux [W]

r = sphere radius [m]

R = radius ratio, $R = \frac{r_e}{r_i}$

Ra = modified Rayleigh number, $Ra = \frac{g\beta D^4}{\nu\lambda\alpha} q$

S = surface area of a sphere ($4\pi r^2$)

t = dimensionless time, $t = \frac{\alpha}{D^2}\tilde{t}$

Δt = time step

T = dimensionless temperature, $T = \frac{\lambda}{qD}(\tilde{T} - \tilde{T}_0)$

$\Delta\tilde{T}$ = difference of temperature between the two spheres [K]

U, V = dimensionless velocity components in the transformed plane, $U = \frac{D}{\alpha}\tilde{U}$, $V = \frac{D}{\alpha}\tilde{V}$

x, y = Cartesian coordinates [m]

Greek symbols

α = thermal diffusivity [m^2 s^{-1}]

β = thermal expansion coefficient [K^{-1}]

η, θ = bispherical coordinates in the transformed plane

λ = thermal conductivity [W m^{-1} K^{-1}]

ν = kinematical viscosity [m^2 s^{-1}]

Ψ = dimensionless stream function, $\Psi = \frac{1}{\alpha D}\tilde{\Psi}$

Ω = dimensionless vorticity, $\Omega = \frac{D}{\alpha^2}\tilde{\Omega}$

Subscripts

i = internal sphere

e = external sphere

0 = initial time

m = mean

cond = conduction

conv = convection

Superscripts

n = incrementing index of the time evolution

p = incrementing index of the iterative process.

$\overline{X}$ = average value

$\tilde{X}$ = dimensional value

Introduction

In recent decades, natural convection of a fluid enclosed in a spherical annulus located between two vertically eccentric spheres has been investigated experimentally and numerically in many research works, in geophysical applications, in solar energy collectors, in thermal storage systems, in nuclear reactor designs and in many other situations.

Some experimental and theoretical studies in the case of two isothermal concentric spheres or cylinders have been led. Weber *et al.* (1973) studied natural convection to a cooled sphere from an enclosed, vertically eccentric, heated sphere. Powe *et al.* (1975) performed experimental measurements for the vertical circular cylinder with

hemispherical ends in a spherical enclosure. Sarr *et al.* (2001) compare the numerical laminar two-dimensional unsteady natural convection in a partial sector-shaped enclosure submitted to a constant heat flux density and a uniform temperature on the inner cylindrical wall.

Others works concerning only the steady state in the case of concentric spheres have been carried out. Astill *et al.* (1980) and Garg (1992) investigated a numerical solution for natural convection in concentric spherical annuli for radius ratio up to 2.0. Singh and Chen (1980) developed semi-analytical studies at moderate Grashof numbers. Caltagirone *et al.* (1980) highlighted the existence of a multicellular flow at critical Rayleigh number for a radius ratio of 2.0. Ingham (1981) and Fujii *et al.* (1984) conducted a numerical analysis of laminar free convection around an isothermal sphere using a finite difference method.

Numerical studies have been done in the case of the transient flow between two isothermal eccentric spheres (Sanjay and Subrata, 1988) for a Prandtl number equal to 10 and a modified Rayleigh number fixed to $4.0\ 10^4$ (Horn *et al.*, 2004) and for various Prandtl numbers (158, 405 and 720) and modified Rayleigh numbers varying from $5.0\ 10^3$ to $6.0\ 10^5$ and for a variable kinematical viscosity.

Research concerning the transient regime flow between two vertically eccentric spheres with the inner sphere heated by a heat flux of constant density and the outer one maintained isothermal are very limited.

Mathematical approach

Let's consider a Newtonian fluid characterized by a Prandtl number Pr, initially at the constant temperature $\tilde{T}_0$, enclosed in an annular space delimited by two vertically eccentric spheres of radiuses r_i and r_e centred respectively on O_i and O_e (Figure 1).

The eccentricity e of two vertical spheres is defined as the algebraic distance $\overline{O_iO_e}$ separating the two centres of the spheres divided by the hydraulic diameter D. While the centre of the outer sphere is above the one of the inner sphere, e is positive. While the centre of the outer sphere is below the one of the inner sphere, e is negative.

Initially, the fluid inside the enclosure is at uniform temperature. A heat flux of constant density q is suddenly applied to the inner sphere while the outer sphere is maintained isothermal ($\tilde{T} = \tilde{T}_0$). The two spheres being heated differently, a transient natural convection develops inside the enclosed space. A numerical study of this convection is to be carried out. To formulate and solve this problem, it is assumed that:

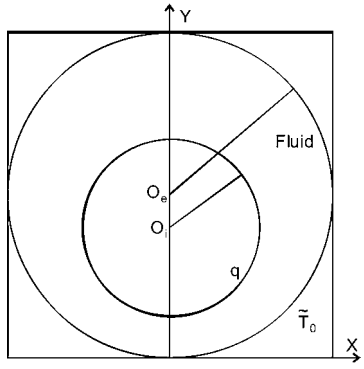

Figure 1.
Geometry of the problem

- the fluid is Newtonian and the flow is laminar. The phenomena are symmetrical with respect to the revolution axis and are two-dimensional;
- all fluid properties are taken to be constant, with the exception of the density in the momentum equation. In this equation, variations of density are due to the differences in temperatures and are thus at the origin of the convection motion. These variations obey the Boussinesq linear law;
- the fluid is non absorbing and temperature gaps between the solid spherical walls are sufficiently low so that the radiation effects are regarded as negligible;
- in the heat equation, the viscous dissipation function as well as the compression effects are neglected.

The vorticity – stream function formalism is used.

Taking into account the geometry of the studied system, it seems more adequate to use a curvilinear coordinates system in which boundary conditions of the domain being studied are given by constant coordinate lines. The bispherical coordinates system is selected. This system constitutes families of eccentric spheres whose centres are located on the symmetrical axis and by horizontal crossed torus passing by poles $+a$ and $-a$.

On a two-dimensional flow consideration basis, the passage from the Cartesian coordinates system (x, y) to the bispheric coordinates one (η, θ) is given by Moon and Spencer (1971):

$$x = a\frac{\sin\theta}{\mathrm{ch}\eta - \cos\theta} \quad \text{and} \quad y = a\frac{\mathrm{sh}\eta}{\mathrm{ch}\eta - \cos\theta} \tag{1}$$

The revolution symmetrical axis is given by equations $\theta = 0$ and $\theta = \pi$. The outer and inner spheres are respectively materialized by lines of coordinates $\eta = \eta_e$ and $\eta = \eta_i$. The governing equations consist of stream function equation, momentum equation and heat equation.

From the above assumption and the coordinate transformation, the governing equation of the bispherical coordinates system can be obtained.

Stream function equation:

$$\Omega = \frac{\Psi}{K^2} - \frac{1}{KH}\left(G_2\frac{\partial\Psi}{\partial\eta} - G_1\frac{\partial\Psi}{\partial\theta}\right) - \frac{1}{H^2}\left(\frac{\partial^2\Psi}{\partial\eta^2} + \frac{\partial^2\Psi}{\partial\theta^2}\right) \tag{2}$$

Momentum and heat equations:
for the momentum equation:

$$\frac{\partial(\Omega/K)}{\partial t} + \frac{1}{H}\left(U - \frac{3Pr.G_2}{K}\right)\frac{\partial(\Omega/K)}{\partial\eta} + \frac{1}{H}\left(V + \frac{3Pr.G_1}{K}\right)\frac{\partial(\Omega/K)}{\partial\theta} = \frac{Pr}{H^2}\left(\frac{\partial^2(\Omega/K)}{\partial\eta^2} + \frac{\partial^2(\Omega/K)}{\partial\theta^2}\right) + \frac{Ra.Pr}{KH}\left(G_2\frac{\partial T}{\partial\eta} - G_1\frac{\partial T}{\partial\theta}\right) \tag{3a}$$

for the heat equation:

$$\frac{\partial T}{\partial t}+\frac{1}{H}\left(U-\frac{G_2}{K}\right)\frac{\partial T}{\partial \eta}+\frac{1}{H}\left(V+\frac{G_1}{K}\right)\frac{\partial T}{\partial \theta}=\frac{1}{H^2}\left(\frac{\partial^2 T}{\partial \eta^2}+\frac{\partial^2 T}{\partial \theta^2}\right) \tag{3b}$$

with:

$$U=\frac{1}{HK}\frac{\partial}{\partial \theta}(K\Psi) \quad \text{and} \quad V=-\frac{1}{HK}\frac{\partial}{\partial \eta}(K\Psi) \tag{4}$$

The associated dimensionless initial and boundary conditions are:

$$t=0:\Omega=0,\Psi=0,T=0,U=V=0 \tag{5}$$

$t > 0$:

(a) inner sphere ($\eta = \eta_i$)

$$\Psi=0,U=V=0 \tag{6}$$

$$\Omega=-\frac{1}{H^2K}\frac{\partial^2(K\Psi)}{\partial \eta^2} \tag{7}$$

$$\frac{\partial T}{\partial \eta}=\frac{a}{D}\frac{ch\eta}{sh^2\eta} \tag{8}$$

(b) outer sphere ($\eta = \eta_e$)

$$\Psi=0,U=V=0 \tag{9}$$

$$\Omega=-\frac{1}{H^2K}\frac{\partial^2(K\Psi)}{\partial \eta^2} \tag{10}$$

$$T=0 \tag{11}$$

(c) axis line segments ($\theta = 0, \theta = \pi$)

$$\frac{\partial \Psi}{\partial \theta}=0,\frac{\partial \Omega}{\partial \theta}=0,\frac{\partial T}{\partial \theta}=0,\frac{\partial U}{\partial \theta}=0,V=0 \tag{12}$$

The local and the average Nusselt numbers relative to the inner and outer spheres are defined by:

$$\text{for the inner sphere: } Nu_i=\frac{1}{T_{i,m}-T_0} \quad \text{and} \quad \overline{Nu}=\overline{Nu_i}=\frac{1}{S_i}\int_{S_i} Nu_i dS_i \tag{13}$$

$$\text{for the outer sphere: } Nu_e=\frac{D\ sh^2\eta_e}{a\ ch\eta_e(T_{i,m}-T_0)}\frac{\partial T}{\partial \eta} \quad \text{and} \quad \overline{Nu_e}=\frac{1}{S_e}\int_{S_e} Nu_e dS_e \tag{14}$$

Numerical formulation

Momentum and heat equations are treated by employing the alternating direction implicit method (ADI) well described by Peaceman and Rach ford (1955), and stream function is solved by using the successive over-relaxation method (SOR) with an optimum relaxation parameter given by the formula of Bejan (1984).

By using the ADI method, vorticity and heat equations generate algebraic systems of equations with tridiagonal matrixes which are solved by Thomas algorithm and iterative procedure (Gourdin and Bourmahrat, 1983).

To ensure a strong stability of iterative numerical calculations and to avoid amplifications of errors, time and space steps allowing coefficients with the same sign for the tridiagonal systems of equations to be obtained, and leading to matrixes with strongly dominant principal diagonals (Euvrard, 1990), were chosen.

In the numerical iterative process, the solution is considered convergent when the relative error between the new and old values of the field variables Q for each time step becomes less than a prescribed criterion (Wu *et al.*, 2004), where Q represents Ψ, T and Ω:

$$\frac{|Q_{new} - Q_{old}|_{max}}{|Q_{new}|_{max}} \leq 10^{-5} \tag{15}$$

The calculated values of Ψ, T and Ω from governing equations become the initial values of the next time step. The steady state solution is reached when the relative error between two consecutive step time values of all field variables inside the studied enclosure is inferior to 0.001 per cent:

$$\frac{|Q^{n+1} - Q_n|_{max}}{|Q_{n+1}|_{max}} \leq 10^{-5} \tag{16}$$

where superscripts n and $n + 1$ indicate the time numerical indexes, respectively at instant t and $t + \Delta t$.

Results and commentaries

For the calculation code to be validated, the case of a thermal natural convection steady state for a Newtonian fluid (air) is studied. This fluid is enclosed in the space situated between two concentric spheres. The outer sphere is maintained at a constant temperature while the inner one is heated by a flux of constant density. The results are compared with those published by Tazi *et al.* (1997). The gaps between these results are less than 3 per cent in relative value (Table I).

An eccentricity equal to 0 being a singularity in the case of vertically eccentric spheres, the value of the eccentricity is fixed to 10^{-3} to obtain the same results as for concentric spheres.

Table I. Comparison of the mean Nusselt number in the case of the inner sphere heated by a flux of constant density for $e = 10^{-3}$, $Pr = 0.7$ and $R = 2$

Ra	10^3	10^4	10^5	10^6	10^7
Nu (Our results)	2.062	3.062	4.977	7.720	12.109
Nu (Tazi *et al.* (1997)	2.098	3.150	5.034	7.794	12.274
Difference (%)	−1.72	−2.8	−1.13	−0.95	−1.34

In order to improve the grid system and the time step value, the sensitivity of these parameters is studied according to the variation of the average Nusselt number relating to the internal wall for a modified Rayleigh number equal to 10^5. The 41×41 grid system and the time step $\Delta t = 10^{-5}$ constituted a good compromise between a low cost in computing times and an acceptable precision (see Tables II and III).

In the present work, the eccentricity varies from -0.6 to $+0.6$ and the modified Rayleigh number from 10^3 to 10^6 for a Prandtl number equal to 0.7 while the ratio of radius is fixed to 2.

Figures 2-4 represent the time evolution of isotherms and streamlines for values of the eccentricity varying from -0.6 to $+0.4$ and for a modified Rayleigh number Ra equal to 10^6, the radius ratio being fixed to 2;

It is established that, by heating the internal wall, the fluid which is in contact with this wall is of course heated and rises along the internal wall. Then, the fluid comes into contact with the isothermal cold wall and goes down along this wall.

The isotherm lines have a spherical shape at the beginning of the heating (Figures 2(a), 3(a) and 4(a)). They become more and more deformed for all the studied values of the eccentricity according to time (Figures 2 (b)-(d), 3 (b)-(d) and 4 (b)-(d)).

At steady state, the maximum value of the stream function Ψ_{max} increases with the eccentricity. This increase is more important with negative values of eccentricity. With increasing time, it is noted on Figures 2-4, the appearance of a free place emerging at the bottom of the enclosure, which suggests an evolution towards a bi-cellular mode. That shows that the convection motion is reinforced with positive eccentricities.

The displacement of the fluid vortex centre to the top when the eccentricity increases, is noted consistently.

Grid system	21×21	21×41	41×41	41×61	61×61	61×91
Nu	4.943	4.940	4.804	4.8020	4.775	4.770
Difference (%)	−3.63	−3.56	−0.71	−0.67	0.10	0.00
Computing time (min)	1	2	8	13	23	38

Table II. Comparison of the mean Nusselt number in the case of the inner sphere heated by a flux of constant density for $e = 10^{-3}$, $Pr = 0.7$ $Ra = 10^5$ and $R = 2$ for different grid systems and for time step $\Delta t = 10^{-4}$

Time steps	10^{-4}	10^{-5}	10^{-6}
Nu	4.804	4.982	5.037
Difference (%)	−4.76	−1.19	0.00
Computing time (min)	8	35	215

Table III. Comparison of the mean Nusselt number in the case of the inner sphere heated by a flux of constant density for $e = 10^{-3}$, $Pr = 0.7$ and $R = 2$ for different time steps and for a 41×41 grid system

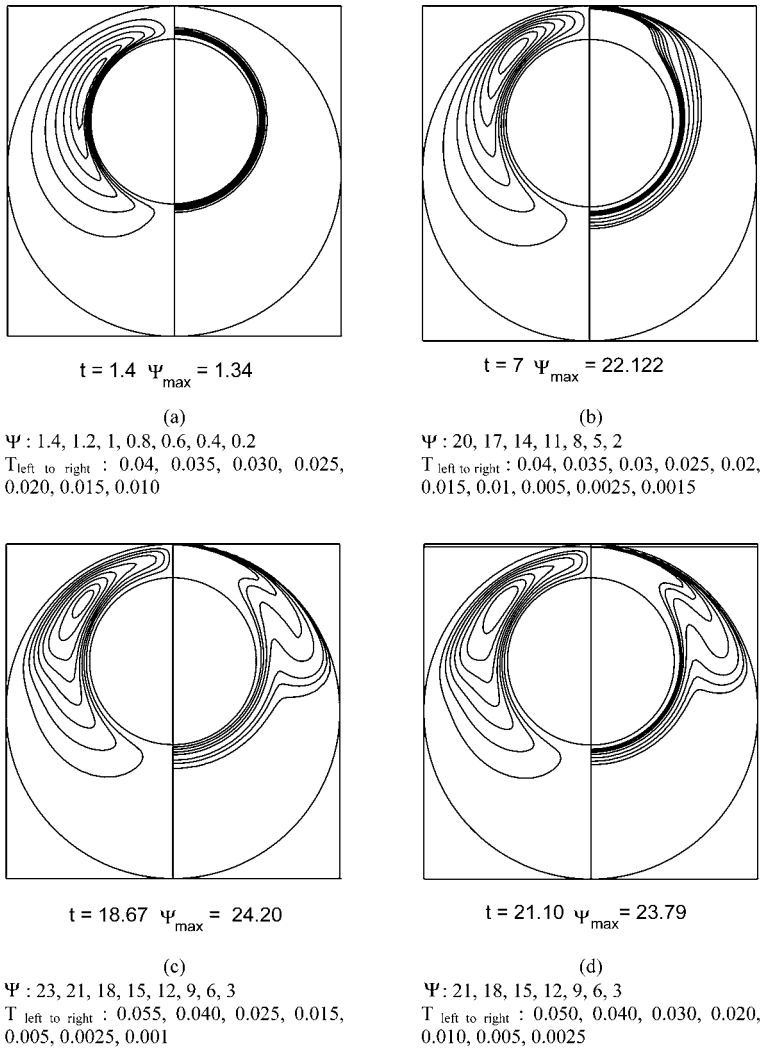

Figure 2.
Evolution of streamlines and isotherms for $Ra = 10^6$, $e = -0.6$, $Pr = 0.7$ and $R = 2$

Figure 5 shows the variation of the dimensionless mean temperature $T_{i,m}$ of the internal sphere, submitted to a heat flux of constant density q, according to dimensionless time for Ra varying from 10^3 to 10^6, $e = 10^{-3}$ and $R = 2$.

From the expressions of the temperature and the modified Rayleigh number Ra, it is possible to write the expression of the dimensionless temperature T according to the heat flux density q applied on the internal wall:

$$T = \frac{\lambda(T' - T'_0}{qD} \tag{17}$$

$$q = \frac{v^2 \lambda Pr}{q\beta D^4} Ra \tag{18}$$

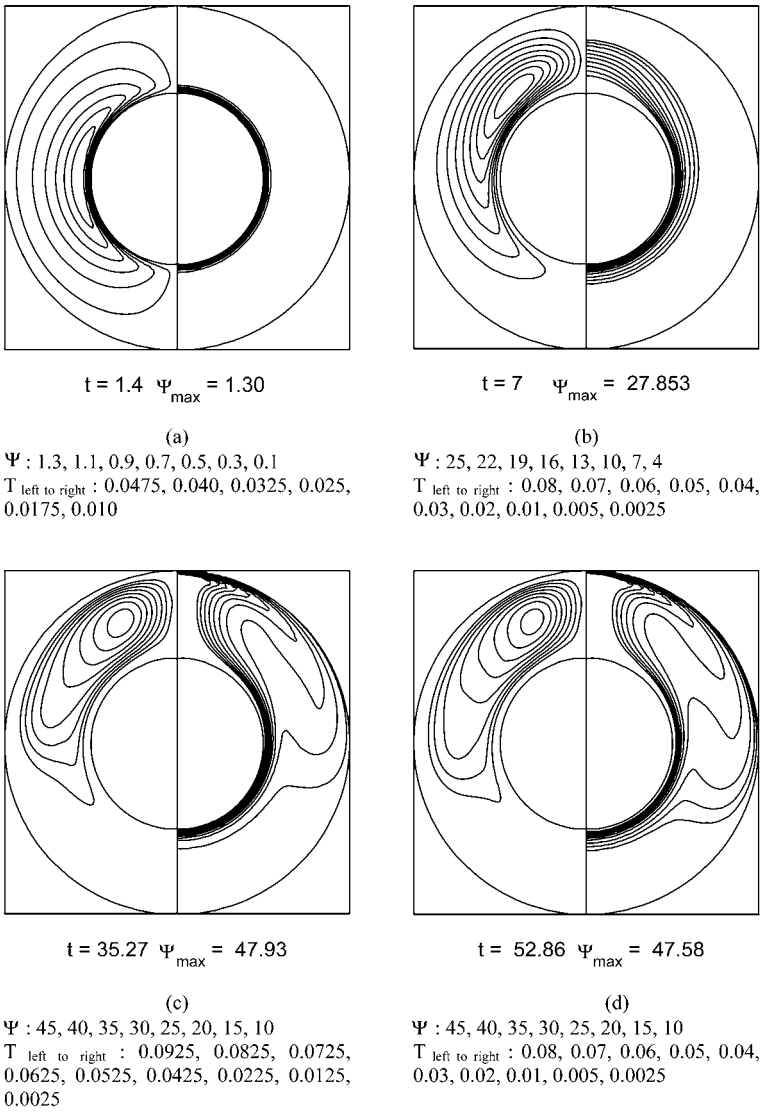

Figure 3.
Evolution of streamlines and isotherms for $Ra = 10^6$, $e = 10^{-3}$, $Pr = 0.7$ and $R = 2$

In general, when the heat flux density q increases the temperature $\tilde{T}$ increases. However, the relative increase of q being higher than that of the difference of temperature $\tilde{T} - \tilde{T}_0$, the definition of the dimensionless temperature shows that T decreases when the heat flux density q increases. Thus, the dimensionless temperature T in an unspecified point inside the studied fluid is inversely proportional to the heat flux density applied on the internal wall and thus to the modified Rayleigh number. This result is confirmed by the analysis of Figure 5 showing the variation of dimensionless mean temperature $T_{i,m}$ of the internal sphere with time for $e = 10^{-3}$ and various values of Ra. The explanation is as follows: when the heat flux density increases, the convection also increases; this involves a greater extraction of heat from

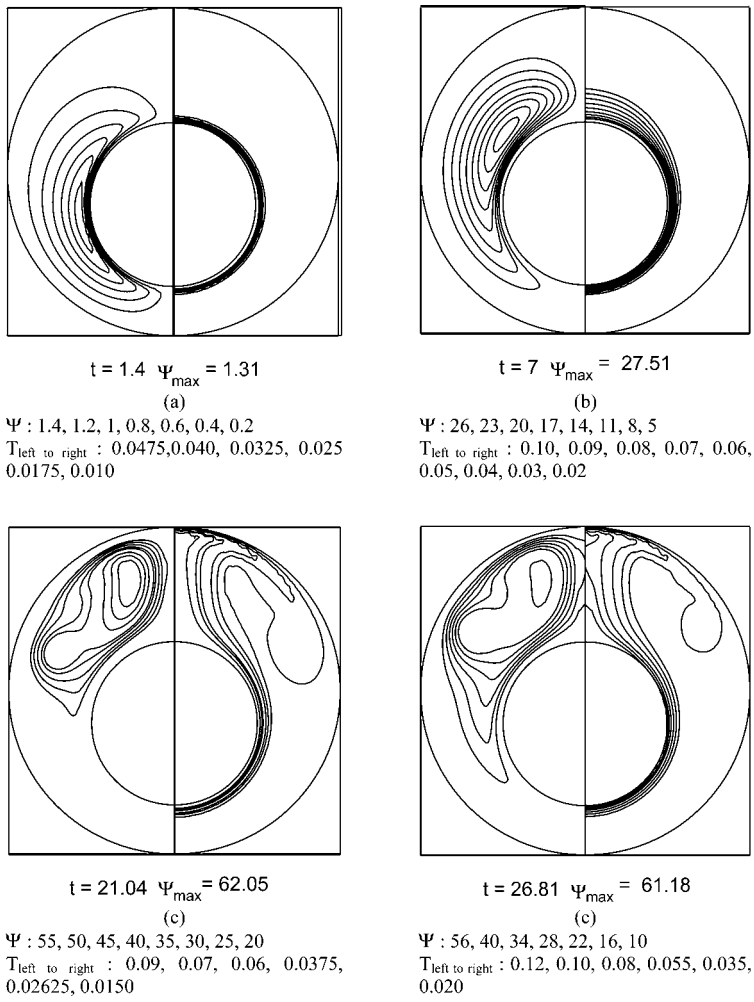

Figure 4.
Evolution of streamlines and isotherms for $Ra = 10^6$, $e = +0.4$, $Pr = 0.7$ and $R = 2$

the internal wall by the fluid in increasing motion and thus, a reduction of this wall temperature.

Figure 6 shows the variations of the maximum value of the stream function Ψ_{max} against dimensionless time for Ra varying from 10^3 to 10^6 while $e = 10^{-3}$ and $R = 2$.

Ψ_{max} increases quickly with time up to a maximum value, then it decreases before stabilizing when the convection steady state is reached. This is explained by the fact that at the beginning of the process, when the heating starts, the phenomena of conduction are more important but with time, the convection motion becomes dominant. The steady state is established and then the fluid motion is stabilized.

It is also noted that the maximum value of the stream function Ψ_{max} increases in the same direction as Ra and as the heat flux density applied to the internal sphere.

Figure 7 represents the variations of the average Nusselt number on the internal sphere, submitted to a heat flux of constant density, against dimensionless time t for values of Ra varying from 10^3 to 10^6, with $e = 10^{-3}$ and $R = 2$. It is noted that on this

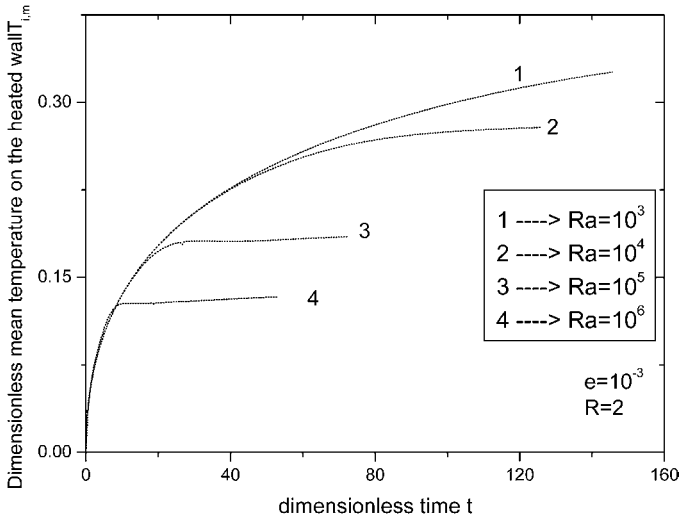

Figure 5.
Variation of dimensionless mean temperature $T_{i,m}$ of the internal sphere with time for $e = 10^{-3}$ and various values of Ra

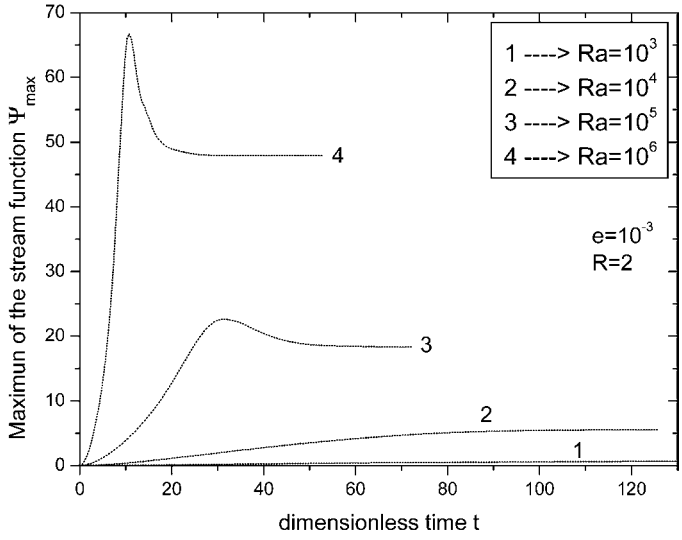

Figure 6.
Variations of the maximum of the stream function Ψ_{max} against dimensionless time for various values of Ra, for $e = 10^{-3}$, and $Pr = 0.7$ and $R = 2$

figure the Nusselt number, which characterizes heat exchange, increases with Ra. The values of average Nusselt numbers $\overline{Nu}_i$ obtained in the case of the internal sphere submitted to a heat flux of constant density while the external sphere is maintained isothermal are more important than those obtained in the case of two isothermal concentric spheres (Bishop *et al.*, 1970; Scanlan *et al.*, 1966; Chu and Lee, 1993).

Figure 8 shows the time evolution of the dimensionless mean temperature $T_{i,m}$ on the heated wall for various values of the eccentricity, for $Ra = 10^6$ and $R = 2$. The dimensionless mean temperature $T_{i,m}$ decreases as the eccentricity increases while remaining negative; this is the case when the centre of the internal sphere is located

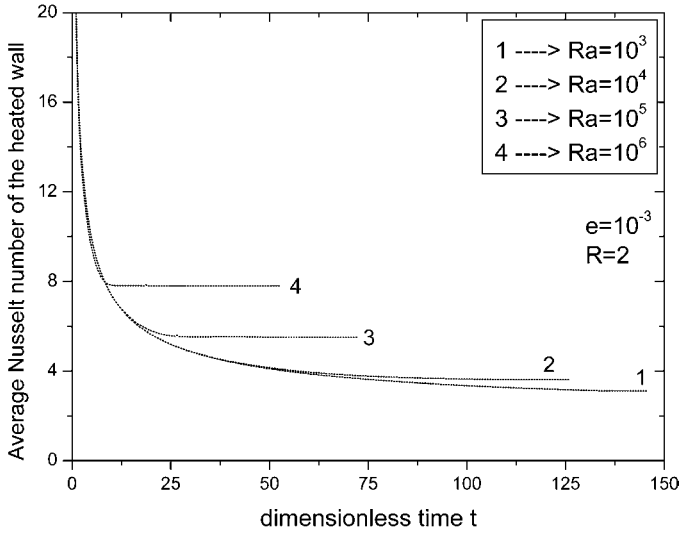

Figure 7.
Variation of average number Nusselt $\overline{Nu_i}$ of the internal sphere according to the dimensionless time t for $e = 10^{-3}$, $Pr = 0.7$ and various values of Ra

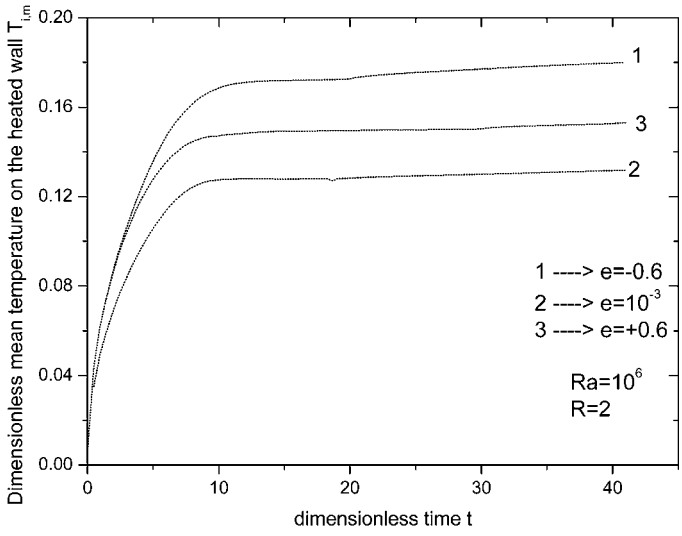

Figure 8.
Time evolution of the dimensionless mean temperature $T_{i,m}$ on the heated wall for $Ra = 10^6$, $R = 2$ and various values of the eccentricity

above the centre of the external one. The result is reversed when the value of the eccentricity is positive and increasing.

Figure 9 shows the time evolution of the maximum value of the stream function Ψ_{max} with various values of the eccentricity. It is noted that the absolute value of Ψ_{max} increases with the eccentricity, which allows us to say that the convection motion is dominant in the heat transfer process.

Figure 10 represents the time evolution of the average Nusselt number $\overline{Nu_i}$ on the internal sphere with various values of the eccentricity, for $Ra = 10^6$.

For great values of dimensionless time, corresponding to the steady state, it is observed that $\overline{Nu_i}$ increases with eccentricity e when this one is negative. It is further

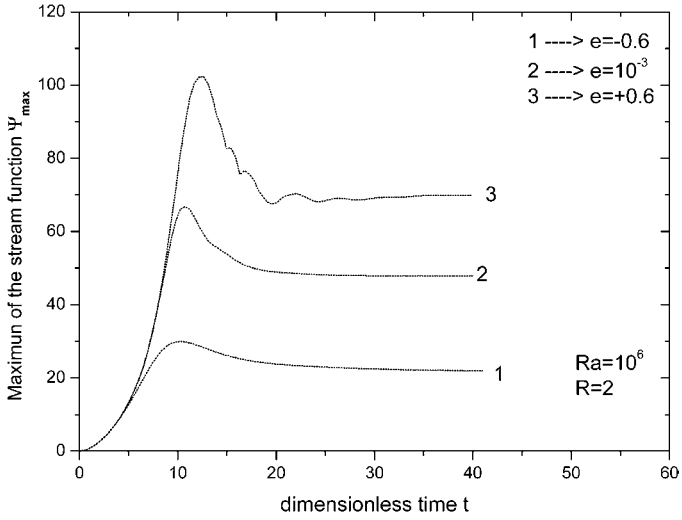

Figure 9.
Variation of the maximum value of the stream function Ψ_{max} according to the dimensionless time t for $Ra = 10^6$, $Pr = 0.7$ and various values of the eccentricity

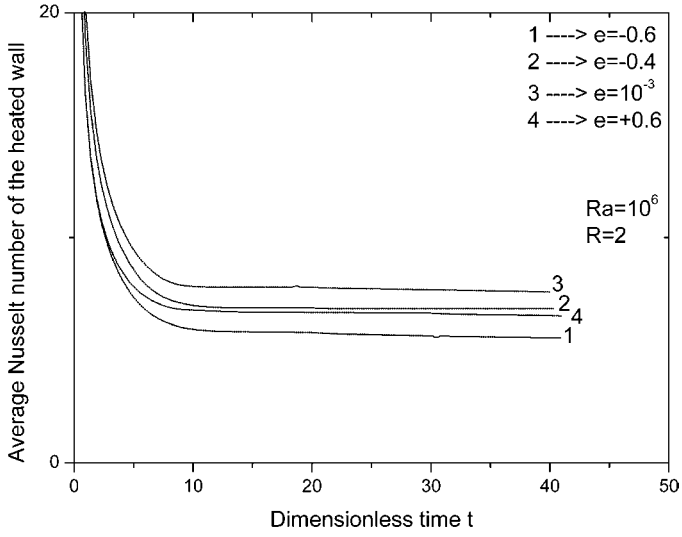

Figure 10.
Variation of the average Nusselt number of the internal sphere $\overline{Nu}_i$ according to the dimensionless time t for $Ra = 10^6$, $Pr = 0.7$ and for various eccentricity values

noted that, for the same absolute values of eccentricity, $\overline{Nu}_i$ is higher for positive values ones. These results are due to the following considerations: when the eccentricity is increasing while remaining negative, the space of containment located in the top level between the two spherical walls becomes larger and the phenomena of convection are more important. In the particular case of quasi concentric spheres ($e = 10^{-3}$), the phenomena of conduction are weaker and the convection becomes the heat transfer dominating mode. The average Nusselt number number $\overline{Nu}_i$ of the internal sphere is consequently more important.

The volume occupied by the fluid between the two spheres increases in the same direction as the radius ratio R. On Figures 11 and 12, it is noted that the dimensionless

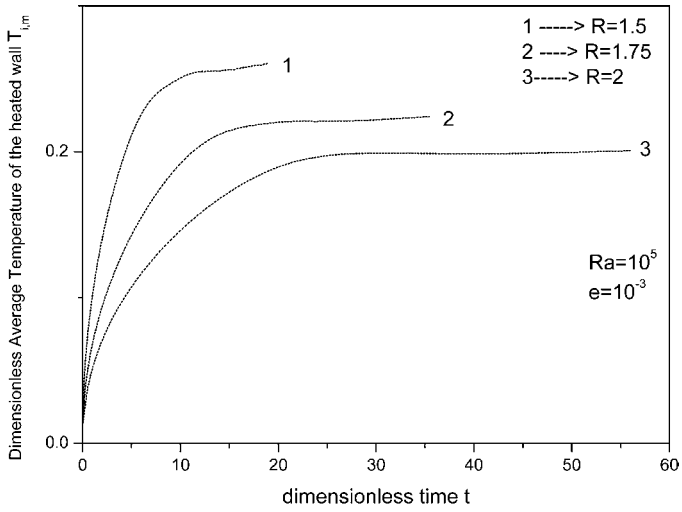

Figure 11.
Variation of the dimensionless average temperature of the heated wall according to the dimensionless time t for $Ra = 10^5$, $Pr = 0.7$ and for various radius ratios R

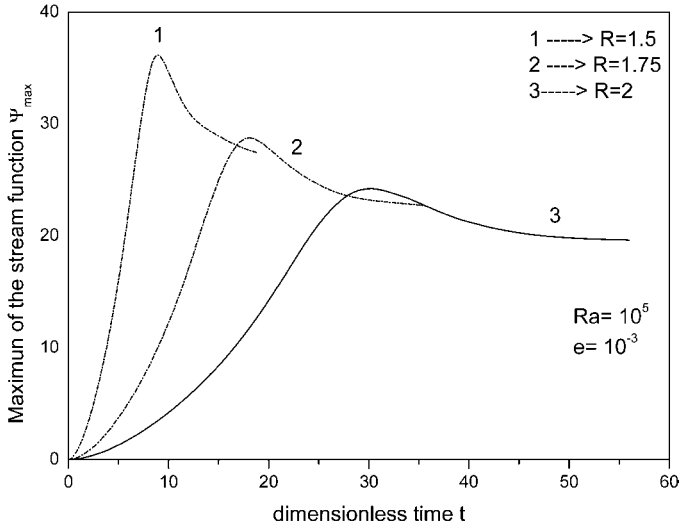

Figure 12.
Variation of the maximum of the stream function according to the dimensionless time t for $Ra = 10^5$, $Pr = 0.7$ and for various radius ratios R

average temperature of the heated wall and the maximum value of the stream function decrease when the radius ratio R increases. Indeed the increase in the volume of fluid involves a much more important energy exchange due to the convection. This energy transfer is established between the surface of the heated wall and the main fluid. This consequently involves a deceleration of the fluid motion.

When the radius ratio R is decreasing the thermal balance is established more quickly. The evolutions of the dynamic field show that the fluid motion intensifies with time increasing until the time corresponding to the establishment of thermal balance. This phase of acceleration is followed by a phase of relaxation, the duration of which increases with R. The variations of the Nusselt number on the heated wall represented on Figure 13 confirm that heat exchange increase with R.

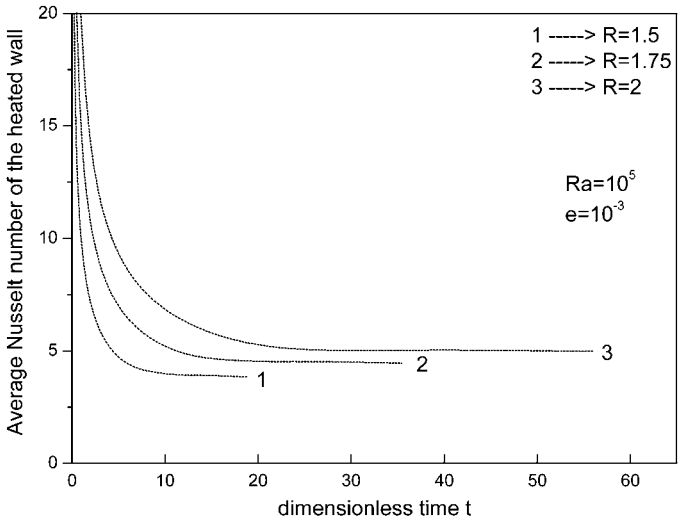

Figure 13.
Variation of the average Nusselt number of the heated wall according to the dimensionless time t for $Ra = 10^5$, $Pr = 0.7$ and for various radius ratios R

Conclusion

By using the bispherical coordinates and finite difference methods such as ADI and SOR, the effects of eccentricity and modified Rayleigh number effects in transient natural convection between vertically eccentric spheres have been studied.

The numerical study has shown that in this case, parameters of the fluid depend strongly of the modified Rayleigh number as well as of the eccentricity.

The isotherm lines and the streamlines have been represented. The study of the stream function and the Nusselt number shows that the convection motion is reinforced for the geometries characterized by positive values of the eccentricity with heat exchange increasing.

We also note that the Nusselt number, which characterises heat exchange, increases with the modified Rayleigh number Ra. The heat exchange also increases with the radius ratio R.

The results show that the steady state is reached faster when the modified Rayleigh number increases and the influence of the eccentricity is very low on the establishment of the steady state.

References

Astill, K.N., Leong, H. and Martorana, R. (1980), "A numerical solution for natural convection in concentric spherical annuli", *Proceedings of the 19th National Heat Transfer, ASME HTD*, Vol. 8, pp. 105-13.

Bejan, A. (1984), *Convection Heat Transfer*, A Wiley-Interscience Publication, John Wiley & Sons, New York, NY.

Bishop, E.H., Mack, L.R. and Scanlan, J.A. (1970), "Natural convection heat transfer between concentric spheres", *International Journal of Heat and Mass Transfer*, Vol. 13, pp. 1857-72.

Caltagirone, J.P., Combarnous, M. and Mojtabi, A. (1980), "Natural convection between two concentric spheres: transition toward a multicellular flow", *Numerical Heat Transfer*, Vol. 3, pp. 107-14.

Chu, H.S. and Lee, T.S. (1993), "Transient natural convection heat transfer between concentric spheres", *International Journal of Heat and Mass Transfer*, Vol. 36, pp. 3159-70.

Euvrard, D. (1990), *Résolution Numérique des Equations aux Dérivées Partielles*, 2nd ed., Masson, Paris.

Fujii, T., Honda, T. and Fujii, M. (1984), "A numerical analysis of laminar free convection around an isothermal sphere: finite difference solution of Navier-Stokes and energy equations between concentric spheres", *Numerical Heat Transfer*, Vol. 7, pp. 103-11.

Garg, V.K. (1992), "Natural convection between concentric spheres", *International Journal of Heat and Mass Transfer*, Vol. 35, pp. 1935-45.

Gourdin, A. and Bourmahrat, M. (1983), *Méthodes Numériques Appliquées*, Lavoisier TEC&DOC, Paris.

Horn, W.W., Tsai, W.C. and Chou, H.-M. (2004), "Transient natural convection heat transfer of fluids with variable viscosity between concentric and vertically eccentric spheres", *International Journal of Heat and Mass Transfer*, Vol. 47, pp. 1685-700.

Ingham, D.B. (1981), "Heat transfer by natural convection between spheres and cylinders", *Numerical Heat Transfer*, Vol. 4, pp. 53-67.

Moon, P. and Spencer, D. (1971), *Field Theory Handbook*, Springer, Berlin.

Peaceman, D.W. and Rachford, H.H. (1955), "The numerical solution of parabolic and elliptic differential equations", *Journal of the Society for Industrial and Applied Mathematics*, Vol. 3 No. 1, pp. 28-41.

Powe, E., Baughman, R.C., Scanlan, J.A. and Teng, J.T. (1975), "Free convection flow patterns between has body and its spherical enclosure", *ASME Journal of Heat Transfer*, Vol. 97, pp. 296-8.

Sanjay, K.R. and Subrata, S. (1988), "A numerical study of natural convection heat transfer in has vertically eccentric spherical annulus", *International Communications in Heat and Mass Transfer*, Vol. 15, pp. 615-26.

Sarr, J., Sall, M., Kane, M.M., Ba, B. and Daguenet, M. (2001), "Numerical natural convection in a sector-shaped enclosure", *International Journal of Numerical Methods for Heat and Fluid Flow*, Vol. 11 No. 4, pp. 342-57.

Scanlan, J.A., Bishop, E.H. and Powe, R.H. (1966), "Heat transfer by natural convection between concentric spheres", *International Journal of Heat and Mass Transfer*, Vol. 9, pp. 649-62.

Singh, S.N. and Chen, J. (1980), "Numerical solution for free convection between concentric spheres at moderate Grashof number", *Numerical Heat Transfer*, Vol. 3, pp. 441-59.

Tazi, M.N.C., Daoudi, S., Le Palec, G. and Daguenet, M. (1997), "Etude numérique du modèle de Boussinesq de convection naturelle laminaire axisymétrique permanente dans un espace annulaire compris entre deux sphères", *Revue Générale de Thermique*, Vol. 36, pp. 239-51.

Weber, N., Powe, R.E., Bishop, E.H. and Scanlan, J.A. (1973), "Heat transfer by natural convection between vertically eccentric spheres", *ASME Journal of Heat Transfer*, Vol. 95, pp. 47-52.

Corresponding author
Mamadou Lamine Sow can be contacted at: mlsow@ucad.sn